Hydrodynamic Properties and Quaternary Structure of the 90 kDa Heat-Shock Protein: Effects of Divalent Cations

Cyrille Garnier,[‡,§] Pascale Barbier,[‡] François Devred,[‡] German Rivas,[||] and Vincent Peyrot*[,‡]

Faculté de Pharmacie, UMR-CNRS 6032, 27 Boulevard Jean Moulin, 13385 Marseille Cedex 5, France, and Centro de Investigaciones Biologicas, Consejo Superior de Investigaciones Cientificas, Velazquez 144, 28006 Madrid, Spain

Received February 7, 2002

ABSTRACT: The 90 kDa heat-shock protein (Hsp90) is one of the major stress proteins whose overall structure remains unknown. In this study, we investigated the influence of divalent cations Mg^{2+} and Ca^{2+} on the hydrodynamic properties and quaternary structure of Hsp90. Using analytical ultracentrifugation, size-exclusion chromatography, and polyacrylamide gel electrophoresis, we showed that native Hsp90 was mostly dimeric. The Hsp90 dimer had a sedimentation coefficient, $s_{w,20}°$, of 6.10 ± 0.03 S, which slightly deviated from the hydrodynamics of a globular protein. Using chemical cross-linking and analytical ultracentrifugation, we showed that Mg^{2+} and Ca^{2+} induced a tertiary conformational change of Hsp90, leading to a self-association process. In the presence of divalent cations, Hsp90 existed as a mixture of monomers, dimers, and tetramers at equilibrium. Finally, to identify Hsp90 domains involved in this divalent cation-dependent self-association, we studied the oligomerization state of the N-terminal (positions 1−221) of Hsp90, the influence of an N-terminal specific ligand, geldanamycin (GA), and the effect of C-terminal truncation on the ability of Hsp90 to oligomerize in the presence of divalent cations. We previously showed that GA inhibits Hsp90 heat-induced oligomerization [Garnier, C., Protasevich, I., Gilli, R., Tsvetkov, P., Lobachov, V., Peyrot, V., Briand, C., and Makarov, A. (1998) *Biochem. Biophys. Res. Commun. 249*, 197−201], but now we observed that GA does not influence divalent cation-dependent oligomerization of Hsp90, suggesting another mechanism. This mechanism involved the C-terminal part of the protein since C-terminally truncated Hsp90 did not oligomerize in the presence of divalent cations.

Heat-shock protein 90 (Hsp90)[1] is one of the most abundant cytosolic proteins in eukaryotic cells, amounting to 1−2% of soluble proteins (*1*, *2*). This level further increases when cells are exposed to stresses such as heat shock, amino acid analogues, and heavy metals (*3*). Hsp90 is required for cell survival and plays a crucial role in many cellular processes (*4*, *5*) by forming transient or stable complexes with several key proteins involved in signal transduction, including protooncogenic protein kinases and nuclear receptors (for a review, see ref *6*). Hsp90 also interacts with cellular structure elements (*7*−*10*) and exhibits conventional chaperone functions (*11*−*14*). The molecular chaperone Hsp90 works in association with other proteins in vivo and in vitro, some of them also members of the Hsp family (*15*).

Two Hsp90 isoforms encoded by separate genes are present in the cytosol of mammalian cells. These isoforms, namely α and *β*, are highly homologous (85%) (*16*). Hsp90α exists predominantly as a homodimer and Hsp90*β* as a monomer (*17*). The dimeric state seems to be required for Hsp90 function. The dimerization of Hsp90α is mediated by the 200 C-terminal amino acids (*18*, *19*), and not by the N-terminal domains, which point in the opposite direction (*20*). These well-conserved N- and C-terminal domains are connected by a highly charged hinge region (*6*, *21*) that seems to play an important role in the regulation of Hsp90 function (*22*). Crystallographic studies have unambiguously shown that the 25 kDa N-terminal domain contains the common binding site for ATP and/or the ADP−Mg complex and geldanamycin (*23*−*25*). It has been suggested that the predominant forms of Hsp90 in cytosolic extracts are oligomers larger than dimers (*26*). On the other hand, in purified preparations of Hsp90, dimers are the major species; oligomers are induced by heat treatment. Both processes (dimerization and oligomerization) seem to be mediated by the 200 C-terminal amino acids (*27*). The heat-induced oligomerization is inhibited by nucleotides and geldanamycin and is activated by various cofactors such as divalent cations and transition metal oxyanions (*28*−*31*).

Recent studies indicated that, as the temperature increases, the ATP−Mg complex leads to the formation of O-ring-shaped structures. This formation is mediated by N-terminal intramolecular interactions for low Hsp90 concentrations. For higher concentrations, intermolecular interactions lead oligo-

* To whom correspondence should be addressed: Faculté de Pharmacie, UMR-CNRS 6032, 27 bd. Jean Moulin, 13385 Marseille Cedex 5, France. Telephone: 491835505. Fax: 491782024. E-mail: vincent.peyrot@pharmacie.univ-mrs.fr.

‡ UMR-CNRS 6032.

§ Present address: Université de Rennes 1, Campus Beaulieu CNRS-UMR 6026 Equipe ATIPE "Structure et Dynamique du Cytosquelette", 35042 Rennes Cedex, France.

|| Consejo Superior de Investigaciones Cientificas.

[1] Abbreviations: Hsp, heat-shock protein; ATP, adenosine triphosphate; ADP, adenosine diphosphate; AUC, analytical ultracentrifugation; SEC, size-exclusion chromatography; EDC, *N*-[3-(dimethylamino)-propyl]-*N*′-ethylcarbodiimide hydrochloride; SDS, sodium dodecyl sulfate; PAGE, polyacrylamide gel electrophoresis; HMW, high-molecular mass marker; MALDI, matrix-assisted laser desorption/ionization; GA, geldanamycin.

10.1021/bi025650p CCC: $22.00
Published on Web 09/07/2002

merization through N-terminal interactions (*20*, *21*, *31*). The ATP−Mg complex induces large Hsp90 conformational changes (*32*). These structural changes were attributed to the binding of ATP. Note that all these works were done with millimolar concentrations of Mg^{2+}. We can easily conceive that Mg^{2+} contributes to these structural changes; for example, the thermal oligomerization of Hsp90 is induced at lower temperatures with millimolar concentrations of Mg^{2+} and Ca^{2+} than without cations (*29*, *33*).

So far, the influence of divalent cations (Mg^{2+} and Ca^{2+}) on Hsp90 had been described only for the temperature-dependent oligomerization (*29*, *33*). Moreover, as Hsp90 oligomerization is associated with Hsp90 chaperone activity (*34*), it is of interest to investigate the influence of these divalent cations on Hsp90 structure under native conditions. Thus, using analytical ultracentrifugation, size-exclusion chromatography, gel electrophoresis, and chemical cross-linking, we studied for the first time the effect of divalent cations on Hsp90 structure under native conditions. With millimolar concentrations of Mg^{2+} and Ca^{2+}, we showed that the mainly dimeric Hsp90 underwent a conformational change associated with a self-association process. Using geldanamycin and equilibrium sedimentation experiments with the Hsp90 N-terminal fragment, we also showed that this domain was not involved in the cation-dependent self-association process, indicating the C-terminal domain plays a crucial role in oligomerization.

MATERIALS AND METHODS

Purification of Hsp90 and Its Recombinant Domain

The 90 kDa heat-shock protein (Hsp90) was purified from porcine brain according to the method of ref *35* modified as described in refs *10* and *29*. Samples were stored at −80 °C. Protein concentrations were determined by UV absorbance with an extinction coefficient of 124 000 ± 6000 M^{-1} cm^{-1} in 10 mM Tris-HCl buffer (pH 7.0) (*10*, *29*). The absorption was corrected for light scattering by the Beckman DU7400 spectrophotometer software. The amino-terminal domain (N-Hsp90) (positions 1−221) was obtained and purified as described by Garnier et al. (*36*).

Analytical Ultracentrifugation

Sedimentation Equilibrium. The experiments were performed with a Beckman Optima XL-A analytical ultracentrifuge equipped with absorbance optics, using an An55Ti rotor. Hsp90 was equilibrated in 10 mM Tris-HCl buffer (pH 7.0) without and with $MgCl_2$ (1, 2, and 5 mM). A short column sedimentation equilibrium experiment (60 mL of Hsp90, loading concentration from 0.05 to 2 mg/mL in the six-channel centerpieces of charcoal-filled Epon) was carried out at two successive speeds (6000 and 10 000 rpm) by taking scans at the appropriate wavelength (230, 250, or 280 nm) when sedimentation equilibrium was reached. The equilibrium temperature was 4 °C. High-speed sedimentation was conducted afterward for baseline correction. Average molecular masses were determined by fitting a sedimentation equilibrium model for a single sedimenting solute to individual data sets with XLAEQ and EQASSOC [supplied by Beckman (*37*)]. Data analysis was also performed by global analysis of several data sets obtained at different loading concentrations using MULTEQ3B and NONLIN, which provided similar results. The partial specific volume of Hsp90 was 0.735 mL/g, calculated from its amino acid composition (ANTHEPROT version 4.0 by G. Deleage).

Sedimentation Velocity. The experiments were carried out at 40 000 rpm and 20 °C in the same XL-A instrument, using 12 mm double-sector centerpieces. Hsp90 (loading concentrations from 0.1 to 4 mg/mL) was equilibrated in 10 mM Tris-HCl buffer (pH 7.0) with the appropriate divalent cation concentration. Apparent sedimentation coefficients were determined using SVEDBERG (*38*) and SEDFIT (*39*)s; similar values of S_{app} were obtained and were corrected to standard conditions using SEDNTERP (*40*). The distributions, $g(s^*)$, were generated by least-squares boundary modeling of sedimentation velocity data by DCDT (*41*, *42*). Similar results were found using SEDFIT. These distributions were then fitted with Gaussian distributions, and the maximum (representing the sedimentation coefficient of the sample) was calculated. A single Gaussian distribution is expected for each monodisperse species in an experiment. The solvent density and the viscosity were calculated with SEDNTERP; they were 0.99851 g/cm^3 and 0.010008 P, respectively (at 20 °C). A gross estimation of the shape of Hsp90 species was determined as follows. The translational frictional coefficient (f) was calculated from the molecular mass and the sedimentation coefficient of Hsp90 determined by equilibrium and velocity analytical ultracentrifugation experiments. The frictional coefficient of the equivalent hydrated sphere (f_o) was estimated using an estimated level of hydration of 0.3 g of H_2O/g of protein (*43*). From these coefficients, the translational frictional ratio (f/f_o) of Hsp90 was determined, and we used Perrin's equation [ELLIPS 1 software (*44*)] to relate the measured values of f/f_0 to axial ratios of the equivalent molecular prolate ellipsoidal model (*45*).

Determination of the Reversibility of the Effect of Magnesium. The Hsp90 sample (5 mg/mL) was incubated with 5 mM Mg^{2+} and then analyzed by sedimentation velocity ultracentrifugation experiments. An identical sample (5 mg/mL with 5 mM Mg^{2+}) was equilibrated in 10 mM Tris-HCl buffer (pH 7.0) through a 15 cm G-25 column to remove the added magnesium. Protein fractions were pooled and separated into two fractions. We added 5 mM Mg^{2+} to one fraction, and the two samples were analyzed by a sedimentation velocity experiment. The protein concentration was ∼1 mg/mL in all the samples.

Hsp90 Cross-Linking Experiments

Chemical cross-linking of Hsp90 was performed using *N*-[3-(dimethylamino)propyl]-*N*′-ethylcarbodiimide hydrochloride (EDC) (Sigma-Aldrich Chemical). The optimal EDC concentration, determined by titration, was 1.5 mM. Hsp90 (1 mg/mL) was incubated for 10 min in 10 mM Tris-HCl buffer (pH 7.0) at room temperature with and without cations. An EDC stock solution (32 mM) in 10 mM Tris-HCl buffer (pH 7.0) was added (5% of the Hsp90 sample volume), and samples were incubated for 30 min at room temperature. The reaction was stopped by 3-fold dilution with buffer (an excess of amine-containing buffer is enough to quench the reaction). Then samples were submitted to polyacrylamide gel electrophoresis (native and SDS−PAGE) or eluted via size-

exclusion chromatography. For experiments in which divalent cations were added after the cross-linking reaction, samples were incubated for an additional 30 min, and then the reaction was stopped as described above.

Polyacrylamide Gel Electrophoresis

PhastSystem (Amersham Pharmacia Biotech) was used for polyacrylamide gel electrophoresis (PAGE). For SDS and native conditions, we used 12.5 and 7.5% homogeneous gels and 4 to 15% gradient gels. Molecular mass markers were from the HMW electrophoresis calibration kit (669, 440, 232, 140, and 67 kDa) for native PAGE (Amersham Pharmacia Biotech) and from the SDS 6H electrophoresis calibration kit (205, 116, 97, 66, 45, and 29 kDa) for SDS−PAGE. Gels were stained with Coomassie Brilliant Blue.

Size-Exclusion Chromatography

Samples of 12 μM Hsp90 (200 μL) in appropriate buffers were loaded on a Sephacryl S-300 High Resolution column (Amersham Pharmacia Biotech) at a flow rate of 20 mL/h; experiments were carried out at 25 °C. The elution buffer was 10 mM Tris-HCl (pH 7.0) with or without cations. The elution was followed at 280 nm; fractions of 500 μL were collected and analyzed on 4 to 15% native PAGE using the PhastSystem (Amersham Pharmacia Biotech). The column was standardized as follows; the calibration curve (Stokes radius vs the partition coefficient K_{av}) was obtained with a standard calibration kit of proteins with known molecular masses and Stokes radii (Amersham Pharmacia Biotech) (*46, 47*). The standards were thyroglobulin (M_r = 669 kDa, R_s = 85 Å), ferritin (M_r = 440 kDa, R_s = 61 Å), and catalase (M_r = 232 kDa, R_s = 52.2 Å). Blue Dextran 2000 (Amersham Pharmacia Biotech) was used to determine the column exclusion volume.

Preparation of the Cross-Linked Hsp90 Dimer for Sedimentation Velocity Experiments

Hsp90 (3.5 mg/mL) was cross-linked in 10 mM Tris-HCl buffer (pH 7.0) over the course of 30 min at room temperature. Excess EDC was removed by running the sample through a PD10 column (Amersham Pharmacia Biotech) equilibrated with 10 mM Tris buffer (pH 7.0). Protein fractions were pooled and analyzed by analytical ultracentrifugation (cf. previously) with and without 5 mM Mg^{2+}.

RESULTS

Hydrodynamic Properties and Quaternary Structure of Native Hsp90. To gain insight into the conformational properties and state of association of Hsp90, a combination of size-exclusion chromatography (SEC) and analytical ultracentrifugation experiments was used. Without divalent cations, SEC analysis showed that Hsp90 eluted from a Sephacryl S-300 column as a single and almost symmetrical peak (Figure 1A, profile a) with a Stokes radius of 62 Å (inset of Figure 1A, arrow a). However, the Stokes radius was too large for a globular dimer with a theoretical molecular mass of 169 286 Da; it corresponded in fact to the molecular mass of a globular protein of ~440 kDa (Figure 1A). SEC cannot be used directly for the estimation

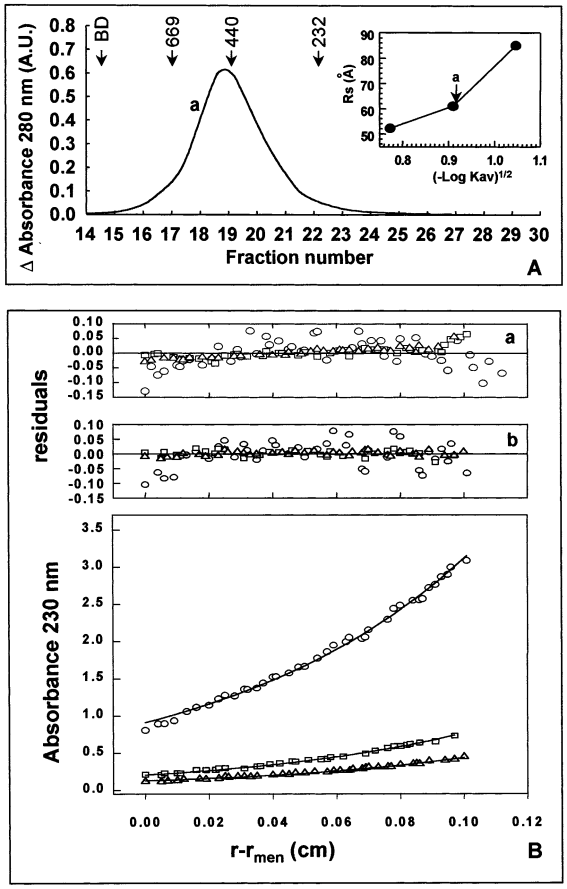

FIGURE 1: Hydrodynamic properties and quaternary structure of native Hsp90. (A) Size-exclusion chromatography. Elution profile of 200 μL of Hsp90 (12 μM) through a Sephacryl S-300 HR column equilibrated with Tris-HCl buffer. Arrows indicate the elution volumes of blue dextran 2000 (BD) and of molecular mass markers. In the inset, proteins with known molecular masses and Stokes radii were used for the calibration curve; the circles represent the Stokes radii as a function of the partition coefficient (K_{av}). The arrow denotes the partition coefficient of Hsp90. (B) Sedimentation equilibrium analysis of Hsp90. The symbols show the experimental radial distribution of Hsp90 at sedimentation equilibrium at 0.05 (△), 0.1 (□), and 0.5 (○) mg/mL. The solid lines represent the best-fit curves of the global analysis of multiple sedimentation equilibrium data with the single-ideal species model as described in Materials and Methods at 4 °C. Of six fitted data sets (the three previously indicated protein concentrations at 6000 and 10 000 rpm), only three (10 000 rpm) are shown. The radial distance at the meniscus (r_{men}) for.05 mg/mL Hsp90 is 6.03 cm; r_{men} (0.1 mg/mL) = 6.52 cm, and r_{men} (0.5 mg/mL) = 7.01 cm. The residuals representing the variation between the experimental data and those generated by the fit with a monomer−dimer (a) or a single-dimer species model (b) are shown.

of the molecular mass of proteins; it is suitable only for a rigid globular protein (*47*). Thus, to determine the molecular mass and the association state of Hsp90, sedimentation equilibrium experiments were performed using three initial loading concentrations of Hsp90 and three rotor speeds, resulting in nine data sets. The analysis of each data set separately gave weight-average molecular masses within 144000−175700 Da over a large concentration range (from 0.05 to 0.5 mg/mL), indicating the protein was essentially dimeric in solution. Fitting the three concentration data sets at 10 000 rpm simultaneously by monomer−dimer or single-ideal species models (Figure 1B) showed that the latter model gave the best distribution of residuals and the minimum square root of variance (see residual distribution b of Figure

Table 1: Hydrodynamic Parameters of Hsp90 and Cross-Linked Hsp90 and the Effect of 5 mM Mg^{2+} [a]

	$S_{20,w}°$ (S)	$S_{20,w}$ (S)	f/f_o	a/b	R_s (Å)	$D_{20,w}°$ (cm^2/s)
Hsp90	6.10 ± 0.03		1.40	4.99	65.0	3.31×10^{-7}
Hsp90 with 5 mM Mg^{2+}		7.72 ± 0.04[b]				
Hsp90 with 5 mM Mg^{2+} re-equilibrated in 10 mM Tris-HCl (pH 7) without Mg^{2+} with 5 mM Mg^{2+}		5.70 ± 0.03[b]				
		7.95 ± 0.04[b]				
cross-linked Hsp90	6.21 ± 0.03		1.38	4.68	63.8	3.36×10^{-7}
cross-linked Hsp90 with 5 mM Mg^{2+}	6.86 ± 0.05		1.25	2.98	57.3	3.71×10^{-7}

[a] The conformational parameters were calculated as described in Materials and Methods, using the theoretical molecular mass of the dimer (169 286 Da) and the partial specific volume values determined from the amino acid composition. $S_{20,w}°$ is the corrected sedimentation coefficient at 20 °C in water. f and f_o are the frictional coefficients. a/b is the axial ratio for the equivalent, hydrated, prolate ellipsoid of revolution. $D_{20,w}°$ is the corrected diffusion coefficient. R_s is the Stokes radius. [b] Apparent sedimentation coefficients of Hsp90 studied by velocity sedimentation (see Materials and Methods).

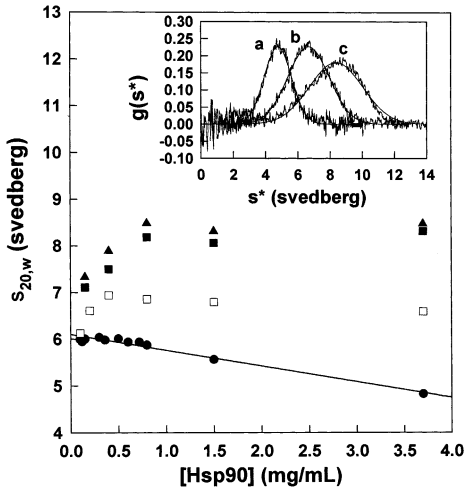

FIGURE 2: Effects of divalent cations on Hsp90. Plot of $S_{20,w}$ values vs Hsp90 concentrations. Hsp90 sedimentation velocities were determined without (●) and with 5 mM Mg^{2+} (■), 5 mM Ca^{2+} (▲), and 2 mM Mg^{2+} (□). The inset shows the apparent sedimentation coefficient distribution computed from the time derivative of the concentration profile by the method of Stafford (*41*): Hsp90 at 3.7 mg/mL alone (a), with 2 mM Mg^{2+} (b), and with 5 mM Mg^{2+} (c). The data were analyzed as described in Materials and Methods; the solid line represents the fitted Gaussian distribution expected for a monodisperse species.

1B). With the single-species model, we found a value of 164 ± 10 kDa, in agreement with the theoretical molecular mass of the dimer (169 286 Da).

Sedimentation velocity experiments confirmed the monodisperse nature of Hsp90 as indicated by the presence of a single sharp boundary. The Hsp90 sedimentation coefficient decreased with concentration [Figure 2 (●)], as expected for a nonassociative single particle, and an $S_{20,w}°$ of 6.10 ± 0.03 S was obtained at infinite dilution. Using this sedimentation coefficient value, we calculated the frictional coefficient ratio (f/f_o) of the Hsp90 dimer to be 1.40 (Table 1), which agrees with that of Iannotti et al. (*48*). Moreover, the time derivative method used in sedimentation velocity experiments and developed by Stafford (*41*) showed an apparent distribution function of $g(s^*)$ versus s^* (inset of Figure 2, curve a) with a single symmetrical peak, confirming the presence of one species. Solution of the $g(s^*)$ plot in terms of a single Gaussian curve gave an s value of 4.77 ± 0.01 S for 3.7 mg/mL Hsp90. Using the error in the Gaussian to obtain the diffusion coefficient, and hence the mass of the species, gave a value of 170 700 Da, corresponding to the mass of the dimer of Hsp90.

Effects of Divalent Cation on Hsp90 Structure. In a previous study, we showed that Hsp90 oligomerized irreversibly around 50 °C (*29*). In the presence of divalent cations, oligomerization occurred around 40−45 °C, suggesting that divalent cations modified Hsp90 structure. Thus, it was of interest to study the effects of Mg^{2+} and Ca^{2+} on Hsp90 structure by sedimentation velocity experiments (Figure 2). Both divalent cations increased the Hsp90 apparent sedimentation coefficient, which rapidly reached 8−9 S. Experiments performed with 2 mM Mg^{2+} gave an intermediate result, between the absence and presence of 5 mM cations (Figure 2). As already mentioned, the presence of 5 mM Mg^{2+} increased the sedimentation coefficient of Hsp90 (1 mg/mL) from ∼5.70 to ∼7.72 S (Figure 2 and Table 1). Running the Hsp90 sample containing Mg^{2+} through a G25 column equilibrated with a magnesium-free buffer to remove the added cation led to an apparent sedimentation coefficient (7.95 S) similar to that of Hsp90 alone (Table 1). This result showed that the Mg^{2+} effect was reversible. These results were not observed with monovalent cations, indicating that divalent cations are specific (data not shown). The sedimentation velocity of a macromolecule depends on its mass, frictional coefficient, and buoyancy (density relative to that of the solvent). Because buoyancy does not change in the presence of divalent cations, the increase in the apparent sedimentation coefficient induced by divalent cations could be due to a self-association process and/or a conformational change. To reveal the distribution of sedimenting species, we used a $g(s^*)$ representation, which is very sensitive for the detection of multiple species. The $g(s^*)$ distribution (inset of Figure 2) of Hsp90 alone (3.7 mg/mL) and with 2 and 5 mM Mg^{2+} showed a large shift toward higher sedimentation coefficients (∼6.67 and ∼8.37 S, respectively) with a large increase in peak width. This peak was not described by a single Gaussian curve, indicating it did not correspond to a single species.

To determine the quaternary structure of Hsp90 in the presence of divalent cations, we performed sedimentation equilibrium experiments. Analysis of the data for a single species showed the weight-average molecular mass ($M_{w,a}$) increased with Hsp90 and cation concentrations (data not shown) to a $M_{w,a}/M_1$ ratio of 3 (M_1 is the theoretical mass of the monomer). Fitting three concentration data sets (0.05, 0.1, and 0.5 mg/mL; Figure 3D) for 10000 rpm simulta-

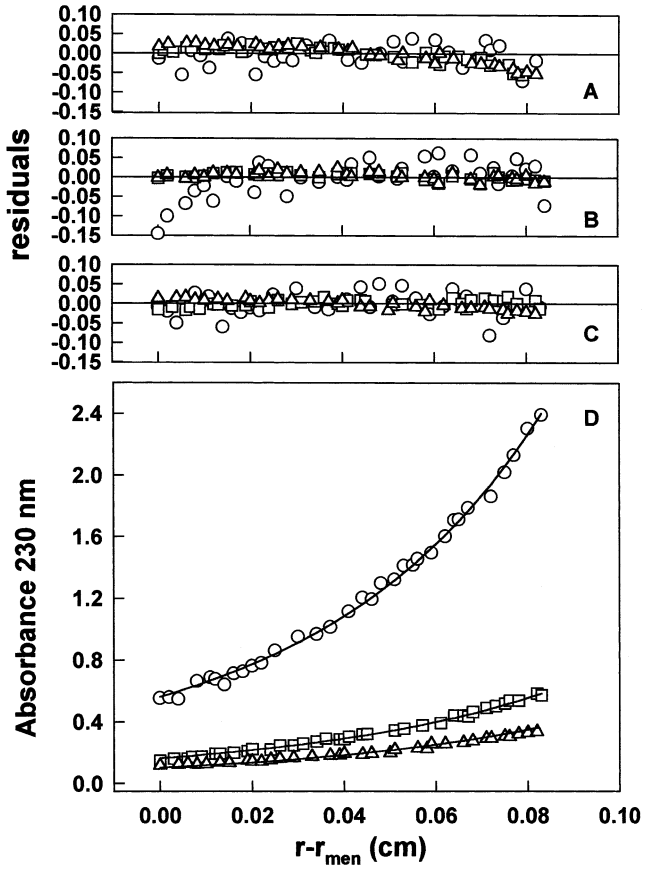

FIGURE 3: Analysis of the effect of 5 mM Mg^{2+} on Hsp90 by sedimentation equilibrium. Equilibrium sedimentation data obtained at 4 °C and 0.05 (△), 0.1 (□), and 0.5 mg/mL (○) at 10 000 rpm were fitted to different models. Shown are the residuals representing the variation between the experimental data and those generated by the fit with a single-ideal species model (A), a monomer−dimer or monomer−dimer−trimer equilibrium model (B), and a monomer−dimer−tetramer equilibrium model (C). In panel D, the symbols show the experimental radial distribution of Hsp90 at sedimentation equilibrium. The solid lines represent the best-fit curve analysis of the global analysis of multiple sedimentation equilibrium data with the monomer−dimer−tetramer equilibrium model [M_1 was constrained to 84 643 Da; $K_{1,2} = (2.34 \pm 1.85) \times 10^7$ M^{-1} and $K_{1,4} = (2.19 \pm 0.05) \times 10^{20}$ M^{-3} for these data].

neously with several models (Figure 3A−C) showed that the monomer−dimer−tetramer model gave the best distribution of residuals and the minimum square root of variance (Figure 3C). Then the values of the dimerization constant $K_{1,2}$ [$(3.0 \pm 1.6) \times 10^7$ M^{-1}] and of the tetramerization constant $K_{1,4}$ [$(1.7 \pm 0.7) \times 10^{20}$ M^{-3}] were determined using three independent determinations.

EDC as a cross-linking agent was also used to check the effects of divalent cations on Hsp90 quaternary structure. First, we monitored the effects of EDC on Hsp90 alone. Figure 4A shows that the cross-linked Hsp90 migrated in native PAGE at a 170−180 kDa band corresponding to the dimer (lane 2). Compared to that of un-cross-linked Hsp90 (lane 1), we observed a weak shift of the dimer band toward lower molecular masses, suggesting that EDC slightly influenced the structure of the Hsp90 dimer. SEC analysis showed the elution profile of cross-linked Hsp90 was similar to that of the un-cross-linked one, but slightly shifted (Figure 4B, profiles a and b). EDC did not induce nonspecific oligomer formation and could thus be used to study the effects of the cation on this protein. Samples treated with

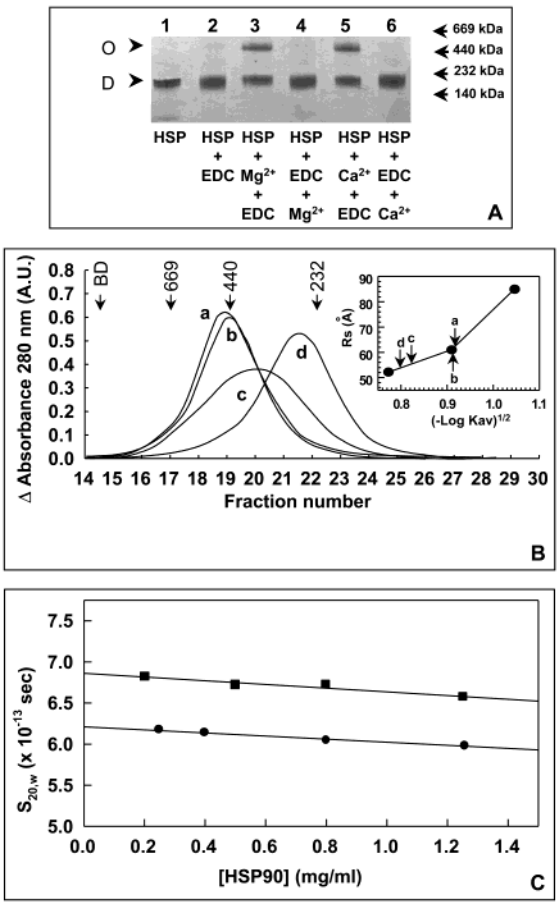

FIGURE 4: Determination of the conformational change induced by divalent cations. (A) Native PAGE analysis. Hsp90 was in lane 1 (6 μM). Hsp90 (6 μM) complexed with EDC was in lane 2. In the other samples, Hsp90 (6 μM) was treated by EDC after and before the addition of 5 mM divalent cations. The order of addition of reagents is indicated below each lane. Samples were analyzed on 4 to 15% gradient native PAGE with the PhastSystem apparatus. D and O indicate migration of dimeric and oligomeric species, respectively, and arrows indicate the position of the molecular mass markers. (B) Size-exclusion chromatography. Elution profile of Hsp90 (a) and cross-linked Hsp90 (b) in the absence of divalent cation; the column was equilibrated with Tris-HCl buffer. (c) Elution profile of cross-linked Hsp90 with 5 mM Mg^{2+}; the column was equilibrated with 5 mM Mg^{2+} and Tris-HCl buffer. (d) Elution profile of 200 μL of cross-linked Hsp90 (12 μM) through a Sephacryl S-300 column. The column was equilibrated with 5 mM Mg^{2+} and Tris-HCl buffer. Arrows indicate the elution volumes of blue dextran 2000 (BD) and of molecular mass markers. In the inset, proteins with known molecular masses and Stokes radii were used for the calibration curve; the circles represent the Stokes radii as a function of the partition coefficient (K_{av}). The arrows denote the partition coefficient of Hsp90 (a), cross-linked Hsp90 (b), Hsp90 with Mg^{2+} and then cross-linked (c), and cross-linked Hsp90 before cation addition and eluted with 5 mM Mg^{2+} (d). (C) Sedimentation velocity of cross-linked Hsp90. Plots of $S_{20,w}$ values vs cross-linked Hsp90 concentrations. After cross-linkage of Hsp90 with EDC, samples were supplemented (■) or not (●) with 5 mM Mg^{2+}. The lines are linear regressions to obtain $S_{20,w}^{\circ}$ values.

EDC, after addition of 5 mM Mg^{2+} or Ca^{2+}, showed two bands in native PAGE (Figure 4A, lanes 3 and 5), corresponding to dimers and oligomers with apparent molecular masses of 180−185 and 470−510 kDa, respectively. Results obtained from Sephacryl S-300 columns equilibrated with 5 mM Mg^{2+} (Figure 4B, profile c) showed that Hsp90 incubated with cations and then cross-linked with EDC eluted as a wide peak, indicating the presence of different species.

So, in the presence of Mg^{2+}, Hsp90 was detected with EDC as oligomers (dimers to higher-order ones). Surprisingly, when cations were added after the cross-linking of Hsp90 with EDC, native PAGE (Figure 4A, lanes 4 and 6) and the Sephacryl S-300 chromatogram (Figure 4B, profile d) clearly showed that the cross-linked Hsp90 did not self-associate, and only dimers were observed in native PAGE. Relative to cross-linked Hsp90 alone (Figure 4, profile b), the presence of ions shifted the elution profile to a lower apparent molecular mass, suggesting a conformational change in the protein.

As previously mentioned, cross-linking of Hsp90 before addition of cations blocked Hsp90 in its dimeric state and inhibited its divalent cation-dependent self-association. Nevertheless, structural changes induced by cations remain possible on cross-linked Hsp90. These results prompted us to study by sedimentation velocity the hydrodynamic properties and the conformational changes induced by Mg^{2+} or Ca^{2+} on the Hsp90 dimer. Figure 4C shows that $S_{20,w}$ of cross-linked Hsp90 with and without 5 mM Mg^{2+} decreased in a linear concentration-dependent manner. This decrease was due to the hydrodynamic nonideality of Hsp90 and fitted well the equation $S_{20,w} = S_{20,w}^{\circ}(1 - gC_T)\ s^{-1}$, where g is the nonideal correction factor, C_T is the protein concentration, $S_{20,w}$ is the sedimentation coefficient corrected for 20 °C in water, and $S_{20,w}^{\circ}$ is the sedimentation coefficient at infinite dilution. Linear regression analysis indicated that dimeric cross-linked Hsp90 sedimented with an $S_{20,w}^{\circ}$ of 6.21 ± 0.03 S without Mg^{2+} and an $S_{20,w}^{\circ}$ of 6.86 ± 0.05 S with 5 mM Mg^{2+}. In both cases, the g value remained constant at 0.033 ± 0.009 mL/mg. Using these sedimentation coefficient values, we calculated (see Materials and Methods) the corresponding translational frictional ratio f/f_o and found a slight decrease in the presence of Mg^{2+} (see Table 1), which indicated a slight increase in Hsp90 compactness in the presence of cations. In summary, cations induced tertiary conformational changes and the oligomerization of Hsp90.

Hsp90 Domains Involved in the Oligomerization Process. Since heat-induced oligomerization started concomitantly with unfolding of the Hsp90 N-terminal domain (*29*, *30*) and since geldanamycin, a specific ligand of the Hsp90 N-terminal domain, inhibited Hsp90 heat-induced oligomerization, it was of interest to test the effect of GA on divalent cation-dependent Hsp90 self-association to determine the domains that are involved. Figure 5A (lane 1b) shows the cross-linked Hsp90 dimer with 3.5×10^{-4} M GA, as compared to Hsp90 alone (lane 1a); no differences were observed. With 5 mM Mg^{2+} (lane 2a) or Ca^{2+} (lane 3a), we observed another band corresponding to oligomeric species. GA did not modify the Hsp90 electrophoretic profile (lanes 2b and 3b), suggesting either that GA binding did not alter the interface involved in oligomerization enhanced by cations or that the N-terminal domain of Hsp90 did not participate in the oligomerization. To determine the process, sedimentation equilibrium experiments were performed on the purified N-terminal Hsp90 domain (positions 1−221). The use of three loading concentrations at three speeds showed this Hsp90 fragment was monomeric in solution. Global analysis of three concentrations at one speed using the one-species model converged to the value of 26.4 ± 2.3 kDa, highly compatible with that previously found (*36*) and with the theoretical molecular mass of the monomer (27.8 kDa).

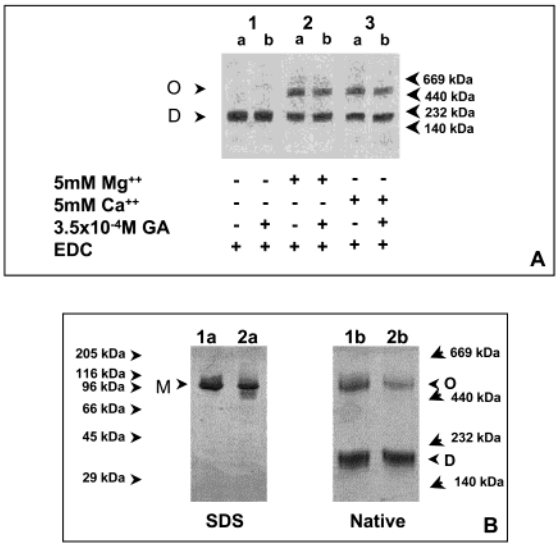

FIGURE 5: Domains of Hsp90 involved in the oligomerization enhanced by divalent cations. (A) Effects of geldanamycin (GA), an N-terminal specific ligand, on 6 μM Hsp90 self-association. The presence and the absence of reagents is indicated with + and −, respectively. Concentrations are indicated at the left. In all experiments, the last compound that was added was EDC. Samples were analyzed on 4 to 15% gradient native PAGE with the PhastSystem apparatus. D and O indicate migration of dimeric and oligomeric species, respectively, and arrows indicate the migration position of the molecular mass markers. (B) C-Terminally truncated Hsp90 oligomerized less than the untruncated form. Homogeneous 12.5% SDS−PAGE analysis of native (lane 1a) and truncated Hsp90 (lane 2a). Homogeneous 7.5% native PAGE analysis of untruncated and truncated Hsp90 with 5 mM Mg^{2+} (lanes 1b and 2b, respectively) and cross-linked with EDC. The Hsp90 concentration was 6 μM. SDS−PAGE and native PAGE were performed with the PhastSystem device. M, D, and O indicate migration of monomeric, dimeric, and oligomeric species, respectively, and arrows indicate the migration position of the molecular mass markers.

Similar experiments were performed with 5 mM Mg^{2+}; a molecular mass of 26.2 ± 1.1 kDa was found. This result indicated that the N-terminal domain of Hsp90 was not involved in the oligomerization induced by cations.

With Hsp90-deleted species, Nemoto implicated the 200 C-terminal amino acids in Hsp90 oligomerization (*27*). Hsp90 has an intrinsic peptidase activity, leading to a 73 kDa truncated product in which the last 150 C-terminal amino acids are missing (*49*). We examined the ability of C-terminally truncated Hsp90 to form oligomers. Figure 5B shows SDS−PAGE comparison between Hsp90 (lane 1a) and Hsp90 incubated for 24 h at 37 °C (lane 2a). For incubated Hsp90, in addition to the intact protein, we observed additional bands of lower molecular masses, which corresponded to truncated products. The two samples, untruncated and the mixture, were incubated with 5 mM Mg^{2+}, treated with EDC, and then analyzed on native PAGE (Figure 5B). As expected for untruncated Hsp90 (lane 1b), we obtained dimeric and oligomeric species. With the Hsp90 mixture (truncated and untruncated) (lane 2b), the number of dimers decreased by 15% and that of oligomers by more than 70%. This indicated that truncated Hsp90 was less able to oligomerize than untruncated Hsp90. However, the inhibition of Hsp90 oligomerization was not complete, due to the presence of untruncated Hsp90 molecules (Figure 5B, lane 2a). Our results suggested that as for dimerization, the

C-terminal domain could participate in divalent cation-dependent self-association of Hsp90.

DISCUSSION

The results give new and complementary information concerning Hsp90 structure in solution and the effects of divalent cations such as Mg^{2+} and Ca^{2+}. Native PAGE showed that Hsp90 was essentially a dimer. Size-exclusion chromatography and sedimentation velocity experiments with native and cross-linked Hsp90 showed that the hydrodynamic behavior of the Hsp90 dimer deviated from that of a rigid globular protein. In agreement with previous works (*48*, *50*) we found a sedimentation coefficient of 6.10 ± 0.03 S. Moreover, sedimentation equilibrium experiments confirmed that Hsp90 was a dimer with a molecular mass of 164 kDa. This mass is close to the one determined by MALDI mass spectroscopy (169.9 kDa) after cross-linking with EDC (*51*).

Via SEC−HPLC methods, Richter et al. (*52*) reported the dissociation constant of the dimer of Hsp90 equaled 60 nM. With this constant and for the less concentrated sample in our sedimentation equilibrium experiments (0.05 mg/mL), a mixture of 70% dimer and 30% monomer in equilibrium would be found, but only dimer was observed. This minor discrepancy could be due first to the different methods that were used. Indeed, in analytical ultracentrifugation experiments, the sample is examined in defined solution conditions and the method allows analysis of association behavior without the complications of possible interactions of the macromolecules with a gel matrix or support. Second, Richter et al. (*52*) used recombinant His-tagged Hsp90 instead of the protein purified from bovine brain tissue. It has been reported that the His tag affects the activity and the association properties of the corresponding proteins (*53*−*55*). Last, Richter et al. (*52*) used a buffer containing 150 mM KCl, and it is well-known that the ionic strength influences the association of proteins, which implicates electrostatic interactions (*56*).

In the presence of cations, sedimentation equilibrium showed that Mg^{2+} and Ca^{2+} induced the self-association of Hsp90 into a monomer−dimer−tetramer system. EDC, a cross-linker agent, used before cation addition, blocked Hsp90 in its dimeric form. In this case, the increase in the sedimentation coefficient was due to a tertiary conformational change in the protein. That cross-linking of the Hsp90 dimer blocked the cation-induced oligomerization suggested that Hsp90 needed to dissociate in monomer before its transition into oligomeric forms. Moreover, in a previous work using EDC (*51*), a species at 254 750 Da was observed by MALDI mass spectrometry that corresponds to a trimer of Hsp90. This species could be really present or could be the result of the dissociation of the tetramer also observed by MALDI. In any case, it appeared that cations induced a conformational change in Hsp90, increasing its compactness, which caused the dimer to dissociate and then the monomer to self-associate into oligomers. Thus, the increase in the sedimentation coefficient induced by cations is due to both tertiary and quaternary Hsp90 conformational changes. Now, it becomes clear that the structural change described for Hsp90 in the presence of the ATP−Mg complex (*20*, *21*, *31*, *32*) and attributed only to the binding of ATP must be linked also to the contributions of Mg^{2+} binding.

Geldanamycin, a specific ligand of the N-terminal domain, does not modify the self-association induced by cations. Moreover, sedimentation equilibrium shows that the N-terminal fragment is a monomer and remains in a monomeric state even in the presence of 5 mM Mg^{2+}. These two results demonstrate clearly that the first 221 amino acids were not involved in the oligomerization induced by cations. In contrast, a mixture of untruncated and C-terminally truncated Hsp90 was less able to self-associate. The slight decrease in dimer number could be explained by the inability of the two truncated monomers to dimerize, whereas heterodimerization (truncated and untruncated monomers) remained possible. The greater effect on oligomerization suggested that these heterodimers did not oligomerize. Moreover, in a previous work, we showed a strong aggregation accompanies thermal denaturation for both the C-terminal fragment of Hsp90 (position 446 to the end of the sequence) and the whole protein, in the presence of Mg^{2+}, but not for the N-terminal domain (see Table 2 in ref *36* and Figure 4B). All these arguments show the 150 C-terminal amino acids are involved in the divalent cation-dependent self-association of Hsp90.

Divalent cation-dependent oligomerization seems to be different from thermally induced oligomerization on two points. First, contrary to oligomerization by cations, which leads to the formation of reversible oligomers, oligomerization by temperature induces the formation of irreversible higher-mass oligomers (*29*). Second, thermal oligomerization starts during Hsp90 N-terminal melting, and GA inhibits the process; in contrast, GA does not inhibit cation oligomerization. Despite these differences, there is one common point between these two processes. Divalent cations induce oligomers with an apparent molecular mass in native PAGE of around 500 kDa, and during thermally induced oligomerization of Hsp90 alone, this oligomer is still present even at high temperatures (>70 °C) (*29*). In the presence of divalent cations, Hsp90 thermal oligomerization occurred at lower temperatures than in their absence (i.e., 40−45 °C). This process could result from the sum of two phenomena: (1) an oligomerization implicating the C-terminal domain and leading to oligomeric structures as observed in this study and (2) a marked elevation of Hsp90 chaperone and peptide binding activity, leading to N-terminal homotopic interactions that concomitantly increase the degree of oligomerization. The presence of oligomers with an apparent molecular mass of ∼500 kDa even at high temperatures for Hsp90 alone could be due to N-terminal intramolecular interactions.

We observed that the effect of divalent cations on oligomerization of Hsp90 was large from 1 to 2 mM and reached a maximum for 5 mM divalent cations. The concentration values of resting ionized cytosolic Mg^{2+} in mammalian cells converge around 0.5 ± 0.2 mM (*57*). Moreover, the importance of fluctuations in free Mg^{2+} as a consequence of hormonal stimulation has been underlined by the observation that many enzymes in different biochemical pathways were activated or inhibited by changes in free Mg^{2+} concentrations. For example, free Mg^{2+} affected the activity of G-protein subunits (*58*−*60*). For the G-protein, there are two sites with different affinities. One site has a high affinity and is responsible for nucleotide hydrolysis, and the second site has a lower affinity that allows the hormonal activation of the G-protein. For Hsp90, we suggest a similar scheme. There is a high-affinity site for Mg^{2+} that

corresponds to the ATP−Mg binding site responsible for the binding of ATP (*23*, *24*) and the regulation of ATPase activity (*61*, *62*). The second site, studied in this paper, enhances the self-association process of Hsp90, modulates its tertiary and quaternary structure, and may have an affinity in the millimolar range. This second site would regulate the chaperone function of Hsp90, favoring or inhibiting its interaction with other polypeptides and receptors. To date, calcium has been implicated only in the regulation of the Hsp90 expression level (*63*). On the basis of our results, Ca^{2+} also modifies the conformation and the quaternary structure of Hsp90. In conclusion, we found evidence of the importance of a tertiary conformational change in Hsp90 self-association induced by divalent cations and shed light on the role of these cations in the modulation of Hsp90 functions.

ACKNOWLEDGMENT

We thank Dr. M. Ladjimi (UMR 7631-CNRS, University Pierre & Marie Curie, Paris, France), Dr. M. G. Catelli (CNRS-UPR 1524, ICGM, Paris, France), and Dr. D. Lafitte for discussions. We thank Dr. P. Schuck (National Institutes of Health, Bethesda, MD) for sharing a new version of SEDFIT. We also thank S. Douillard for assistance with protein purification and C. Alfonso with analytical ultracentrifugation analysis.

REFERENCES

1. Lai, B. T., Chin, N. W., Stanek, A. E., Keh, W., and Lanks, K. W. (1984) *Mol. Cell. Biol. 4*, 2802−2810.
2. Lindquist, S., and Craig, E. A. (1988) *Annu. Rev. Genet. 22*, 631−677.
3. Schlesinger, M. J. (1990) *J. Biol. Chem. 265*, 12111−12114.
4. Borkovich, K. A., Farrelly, F. W., Finkelstein, D. B., Taulien, J., and Lindquist, S. (1989) *Mol. Cell. Biol. 9*, 3919−3930.
5. Parsell, D. A., and Lindquist, S. (1993) *Annu. Rev. Genet. 27*, 437−496.
6. Richter, K., and Buchner, J. (2001) *J. Cell. Physiol. 188*, 281−290.
7. Sanchez, E. R., Redmond, T., Scherrer, L. C., Bresnick, E. H., Welsh, M. J., and Pratt, W. B. (1988) *Mol. Endocrinol. 2*, 756−760.
8. Akner, G., Mossberg, K., Sundqvist, K. G., Gustafsson, J. A., and Wikstrom, A. C. (1992) *Eur. J. Cell Biol. 58*, 356−364.
9. Fostinis, Y., Theodoropoulos, P. A., Gravanis, A., and Stournaras, C. (1992) *Biochem. Cell Biol. 70*, 779−786.
10. Garnier, C., Barbier, P., Gilli, R., Lopez, C., Peyrot, V., and Briand, C. (1998) *Biochem. Biophys. Res. Commun. 250*, 414−419.
11. Wiech, H., Buchner, J., Zimmermann, R., and Jakob, U. (1992) *Nature 358*, 169−170.
12. Miyata, Y., and Yahara, I. (1992) *J. Biol. Chem. 267*, 7042−7047.
13. Miyata, Y., and Yahara, I. (1995) *Biochemistry 34*, 8123−8129.
14. Freeman, B. C., and Morimoto, R. I. (1996) *EMBO J. 15*, 2969−2979.
15. Dittmar, K. D., Banach, M., Galigniana, M. D., and Pratt, W. B. (1998) *J. Biol. Chem. 273*, 7358−7366.
16. Hickey, E., Brandon, S. E., Smale, G., Lloyd, D., and Weber, L. A. (1989) *Mol. Cell. Biol. 9*, 2615−2626.
17. Minami, Y., Kawasaki, H., Miyata, Y., Suzuki, K., and Yahara, I. (1991) *J. Biol. Chem. 266*, 10099−10103.
18. Minami, Y., Kimura, Y., Kawasaki, H., Suzuki, K., and Yahara, I. (1994) *Mol. Cell. Biol. 14*, 1459−1464.
19. Nemoto, T., Ohara-Nemoto, Y., Ota, M., Takagi, T., and Yokoyama, K. (1995) *Eur. J. Biochem. 233*, 1−8.
20. Maruya, M., Sameshima, M., Nemoto, T., and Yahara, I. (1999) *J. Mol. Biol. 285*, 903−907.
21. Buchner, J. (1999) *Trends Biochem. Sci. 24*, 136−141.
22. Scheibel, T., Siegmund, H. I., Jaenicke, R., Ganz, P., Lilie, H., and Buchner, J. (1999) *Proc. Natl. Acad. Sci. U.S.A. 96*, 1297−1302.
23. Prodromou, C., Roe, S. M., Piper, P. W., and Pearl, L. H. (1997) *Nat. Struct. Biol. 4*, 477−482.
24. Prodromou, C., Roe, S. M., O'Brien, R., Ladbury, J. E., Piper, P. W., and Pearl, L. H. (1997) *Cell 90*, 65−75.
25. Stebbins, C. E., Russo, A. A., Schneider, C., Rosen, N., Hartl, F. U., and Pavletich, N. P. (1997) *Cell 89*, 239−250.
26. Krishna, P., Reddy, R. K., Sacco, M., Frappier, J. R., and Felsheim, R. F. (1997) *Plant Mol. Biol. 33*, 457−466.
27. Nemoto, T., and Sato, N. (1998) *Biochem. J. 330*, 989−995.
28. Yonehara, M., Minami, Y., Kawata, Y., Nagai, J., and Yahara, I. (1996) *J. Biol. Chem. 271*, 2641−2645.
29. Garnier, C., Protasevich, I., Gilli, R., Tsvetkov, P., Lobachov, V., Peyrot, V., Briand, C., and Makarov, A. (1998) *Biochem. Biophys. Res. Commun. 249*, 197−201.
30. Chadli, A., Ladjimi, M. M., Baulieu, E. E., and Catelli, M. G. (1999) *J. Biol. Chem. 274*, 4133−4139.
31. Wassenberg, J. J., Reed, R. C., and Nicchitta, C. V. (2000) *J. Biol. Chem. 275*, 22806−22814.
32. Csermely, P., Kajtar, J., Hollosi, M., Jalsovszky, G., Holly, S., Kahn, C. R., Gergely, P., Soti, C., Mihaly, K., and Somogyi, J. (1993) *J. Biol. Chem. 268*, 1901−1907.
33. Jakob, U., Meyer, I., Bugl, H., Andre, S., Bardwell, J. C., and Buchner, J. (1995) *J. Biol. Chem. 270*, 14412−14419.
34. Nemoto, T., Ono, T., and Tanaka, K. (2001) *Biochem. J. 354*, 663−670.
35. Yonezawa, N., Nishida, E., Sakai, H., Koyasu, S., Matsuzaki, F., Iida, K., and Yahara, I. (1988) *Eur. J. Biochem. 177*, 1−7.
36. Garnier, C., Lafitte, D., Tsvetkov, P. O., Barbier, P., Leclerc-Devin, J., Millot, J. M., Briand, C., Makarov, A. A., Catelli, M. G., and Peyrot, V. (2002) *J. Biol. Chem. 277*, 12208−12214.
37. Minton, A. P. (1994) in *Modern Analytical Ultracentrifugation* (Schuster, T. M., and Laue, T. M., Eds.) pp 81−93, Birkhauser, Boston.
38. Philo, J. S. (1994) Acquisition and Interpretation of data for biological and synthetic polymer systems, in *Modern Analytical Ultracentrifugation* (Shuster, T. M., and Laue, T. M., Eds.) pp 156−170, Birkhauser, Boston.
39. Schuck, P., and Rossmanith, P. (2000) *Biopolymers 54*, 328−341.
40. Laue, T. M., Shah, B. D., Ridgeway, T. M., and Pelletier, S. L. (1992) in *Analytical Ultracentrifugation in Biochemistry and Polymer Sciences* (Harding, S. E., Rowe, A. J., and Horton, J. C., Eds.) pp 90−125, The Royal Society of Chemistry, Cambridge, U.K.
41. Stafford, W. F., III (1992) in *Analytical Ultracentrifugation in Biochemistry and Polymer Science* (Harding, S. E., Rowe, A. J., and Horton, J. C., Eds.) pp 359−393, The Royal Society of Chemistry, Cambridge, U.K.
42. Stafford, W. F., III (1996*) Biophys. J. 70*, A231.
43. Pessen, H., and Kumosinski, T. F. (1985) *Methods Enzymol. 117*, 219−255.
44. Harding, S. E., Horton, J. C., and Colfen, H. (1997) *Eur. Biophys. J. 25*, 347−359.
45. Perrin, F. (1936) *J. Phys. Radium 7*, 1.
46. Siegel, L. M., and Monty, K. J. (1966) *Biochim. Biophys. Acta 112*, 346−362.
47. Le Maire, M., Rivas, E., and Moller, J. V. (1980) *Anal. Biochem. 106*, 12−21.
48. Iannotti, A. M., Rabideau, D. A., and Dougherty, J. J. (1988) *Arch. Biochem. Biophys. 264*, 54−60.
49. Montel, V., Gardrat, F., Azanza, J.-L., and Raymond, J. (2000) *Life Sci. 67*, 1585−1600.
50. Koyasu, S., Nishida, E., Kadowaki, T., Matsuzaki, F., Iida, K., Harada, F., Kasuga, M., Sakai, H., and Yahara, I. (1986) *Proc. Natl. Acad. Sci. U.S.A. 83*, 8054−8058.
51. Garnier, C., Lafitte, D., Jorgensen, T. J. D., Jensen, O. N., Briand, C., and Peyrot, V. (2001) *Eur. J. Biochem. 268*, 2402−2407.
52. Richter, K., Muschler, P., Hainzl, O., and Buchner, J. (2001) *J. Biol. Chem. 276* (36), 33689−33696.
53. Rosenfeld, S. S., Correia, J. J., Xing, J., Rener, B., and Cheung, H. C. (1996) *J. Biol. Chem. 271*, 30212−30221.
54. Whitby, G. F., Phillips, J. D., Kushner, J. P., and Hill, C. P. (1998)-*EMBO J. 17*, 2463−2471.

55. Geoghegan, K. F., Dixon, H. B., Rosner, P. J., Hoth, L. R., Lanzetti, A. J., Borzilleri, K. A., Marr, E. S., Pezzullo, L. H., Martin, L. B., LeMotte, P. K., McColl, A. S., Kamath, A. V., and Stroh, J. G. (1999) *Anal. Biochem. 267*, 169−184.
56. McDonnell, J., Calvert, R., Beavil, R. L., Beavil, A. J., Henry, A., Jr., Sutton, B. J., Gould, H., Jr., and Cowburn, D. (2001) *Nat. Struct. Biol. 8*, 437−441.
57. Romani, A., and Scarpa, A. (1992) *Arch. Biochem. Biophys. 298*, 1−12.
58. Brandt, D. R., and Ross, E. M. (1986) *J. Biol. Chem. 261*, 1656−1664.
59. Gilman, A. G. (1987) *Annu. Rev. Biochem. 56*, 615−649.
60. Higashijima, T., Ferguson, K. M., Sternweis, P. C., Smigel, M. D., and Gilman, A. G. (1987) *J. Biol. Chem. 262*, 762−766.
61. Csermely, P., and Kahn, C. R. (1991) *J. Biol. Chem. 266*, 4943−4950.
62. Nardai, G., Schnaider, T., Soti, C., Ryan, M. T., Hoj, P. B., Somogyi, J., and Csermely, P. (1996) *J. Biosci. 21*, 179−190.
63. Elo, M. A., Sironen, R. K., Kaarniranta, K., Auriola, S., Helminen, H. J., and Lammi, M. J. (2000) *J. Cell. Biochem. 79*, 610−619.

BI025650P